STUDY OF SCALE FORMATION ON AISI 316L IN SIMULATED SOLID OXIDE FUEL CELL BI-POLAR ENVIRONMENTS

M. Ziomek-Moroz, B.S. Covino, Jr., S.D. Cramer, G.R. Holcomb, S.J Bullard
U.S. Department of Energy, Albany Research Center
P. Singh, C. F. Windisch, Jr., *Pacific Northwest National Laboratory*

ABSTRACT

Significant progress made towards reducing the operating temperature of solid oxide fuel cells (SOFC) from ~1000°C to ~600°C is expected to permit the use of metallic materials with substantial cost reduction. One of the components in a SOFC stack to be made of metallic materials is a bipolar separator, also called an interconnect. It provides electrical connection between individual cells and serves as a gas separator to prevent mixing of the fuel and air. At operating temperature, the material selected for interconnects should possess good chemical and mechanical stability in complex fuel and oxidant gaseous environments, good electrical conductivity, and a coefficient of thermal expansion (CTE) that matches that of the cathode, anode, and electrolyte components. Cr_2O_3 scale-forming alloys appear to be the most promising candidates.

There appears to be a mechanism whereby the environment on the fuel side of a stainless steel interconnect changes the corrosion behavior of the metal on the air side. The corrosion behavior of 316L stainless steel simultaneously exposed to air on one side and H_2+3%H_2O on the other at 907 K was studied using X-ray diffraction (XRD) and Raman spectroscopy. The electrical property of the investigated material was determined in terms of area-specific resistance (ASR). The chemical and electrical properties of 316L exposed to a dual environment of air/ (H_2+H_2O) were compared to those of 316L exposed to a single environment of air/air.

INTRODUCTION

Solid oxide fuel cells (SOFCs) are one of the high-energy conversion devices that generate electricity and heat by electrochemically combining a gaseous fuel and oxidizing gas via an ion-conducting electrolyte. Advances in solid-state manufacturing show the promise for making SOFCs applicable in many power applications. Significant progress has been made in reducing the operating temperature of the SOFC stack from ~1273 K (1000 °C) to ~ 873K (600 °C).[1] With a reduction of operating temperature, metallic materials can be used for the SOFC bipolar separator, i.e., the interconnect, that makes the electrical connection between individual cells and separates fuel and the oxidizer, typically air. There are several advantages of using metals over currently used ceramic materials based on doped $LaCrO_3$: 1) achievement of gas tightness between fuel and air gases, 2) ease of handling, which lowers fabrication cost, 3) high electronic and thermal conductivity, which increases the cell performance.[2]

During operation at high temperatures, oxide scale formation takes place on the metallic material surface as a result of the material reacting with the fuel and atmospheric gases, such as O_2, H_2O, CO, CO_2. In the case of internal reforming of hydrocarbon fuels, CH_4 is also present.[2] Chromium sesquioxide-forming metallic materials appear to be the most promising candidates since they show relatively low electrical resistance, high corrosion resistance, and suitable thermal expansion behavior.[3, 4] Among the Cr_2O_3 - forming alloys, ferritic stainless steels are promising candidates to fulfill the technical and economical requirements. The oxidation behavior of ferritic alloys has been reported by several research groups. However, the investigations were performed in either air or H_2-H_2O atmosphere.[5-7] The oxidation behavior of 304 stainless steel[8] and AISI430[9] at 800 ^oC in a dual environment consisting of fuel (H_2-H_2O) on one side of the metal and air on the other is different from their oxidation behavior solely in air. Similarly, the oxidation behavior of 316L stainless steel in a dual environment is different from its oxidation behavior in air.[10] Authors hypothesize that hydrogen present on the fuel side appears to affect oxidation behavior on the air side.

This paper describes the corrosion behavior of 316L simultaneously exposed to air on one side and a mixture of H_2 and 3% H_2O on the other side at 634 ^oC (907 K). Also, the area-specific resistance (ASR) of the AISI 316L stainless steel exposed to the dual environment is compared to that of AISI 316L stainless steel exposed solely to air.

EXPERIMENTAL

Materials

Commercial AISI 316L stainless steel tubes were the materials studied. The outside and inside surfaces of two tubes were cleaned with acetone. After cleaning, the specimens were installed inside the furnace as shown in Figure 1.

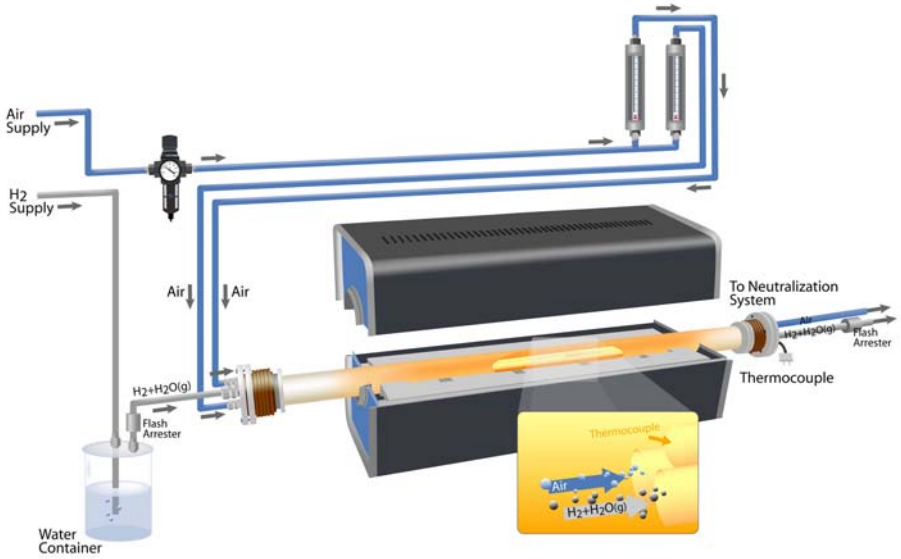

Fig. 1. Experimental setup for tubular specimens.

Corrosion Experiments

One tube was simultaneously exposed to fuel on one side and air on the other side, i.e., a dual environment consisting of H_2 +3% H_2O and air. The second tube was exposed solely to air, i.e., a single environment. The tubes were oxidized at 634 ^oC for 96 h. The fuel was a mixture of H_2 + 3% H_2O prepared by bubbling H_2 through a water container at room temperature.

Area-Specific Resistance Measurements

The area specific resistance (ASR) measurements were conducted at the U.S. Department of Energy, National Energy Technology Laboratory. The ASR measurements were carried out on oxidized 316L using a 2-point probe method. Assuming extremely low/negligible resistance through the steel, the method measured the resistance of the oxide scale and all interfaces. A constant current was used and the resulting voltage across the specimen was measured. Pt- paste electrodes were attached to each side of the oxidized specimen. After the Pt electrodes were attached to the specimen, the experimental assembly was placed in the furnace and heated. The measurements started at 600 ^oC and continued with 50^oC increment up to 900 ^oC. The measurements were conducted in air atmosphere.

Surface Analysis

Surface microstructure and topography of the scale was characterized using scanning electron microscopy (SEM). Scale reaction products formed on the steel surfaces were identified by X-ray diffraction (XRD) and Raman spectroscopy.

RESULTS AND DISCUSSION

Surface Microstructure

Figure 2 shows the microstructure of the scale formed on the 316L tube oxidized in air in the single environment. Both surfaces were covered uniformly with cubic – shape grains. The grain boundaries of the substrate metal were not visible indicating thick oxide scale formation.

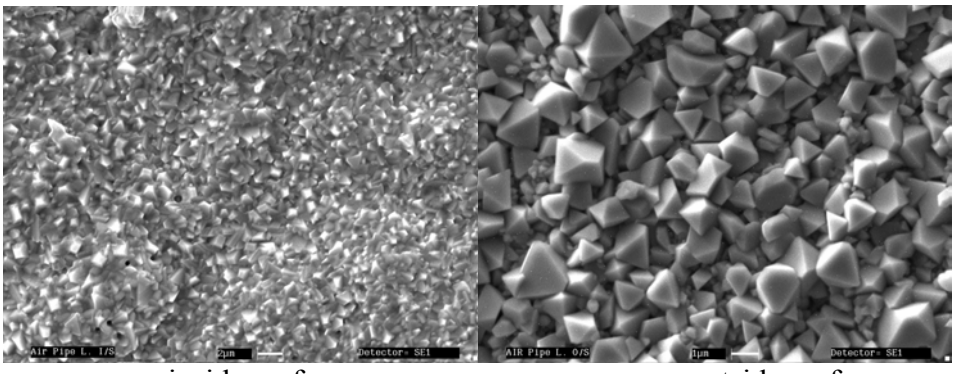

inside surface outside surface

Fig.2. SEM micrographs of scale on 316L surfaces exposed to single environment at 634 ^oC for 96 h.

Figure 3 shows the scale formed on the 316L tube in the dual environment with the outside surface oxidized in air and the inside surface in H_2+3% H_2O. Both surfaces consist of very finely structured scale. It has a distinctly different appearance from that formed in the single environment, apparently lacking the cubic-shaped grains. The scale appears to be relatively thick having both large-scale and very small-scale structure.

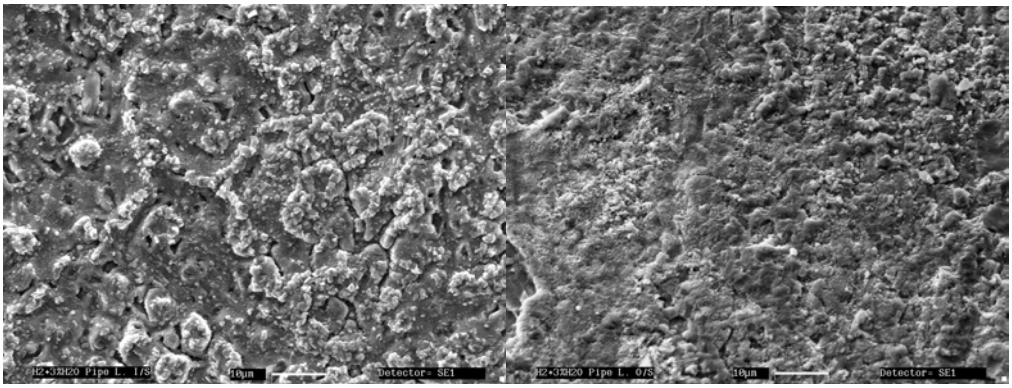

inside surface : H_2+3% H_2O outside surface: air

Fig. 3. SEM micrographs of scale on 316L surfaces exposed to dual environment at 634 ^oC for 96 h.

Phases in Oxide Scales

The phases formed on the 316L stainless steel tubes in single and dual environment and identified by in-situ XRD are given in Table 1. Figure 4 shows the XRD pattern for the outside surface of the single environment specimen. The identified phases are Fe_3O_4 spinel and Cr_2O_3. The phases identified in the scale formed inside the tubular specimen are Fe_2O_3, $(Fe,Cr)_2O_3$, and Fe_3O_4 spinel, Figure 5.

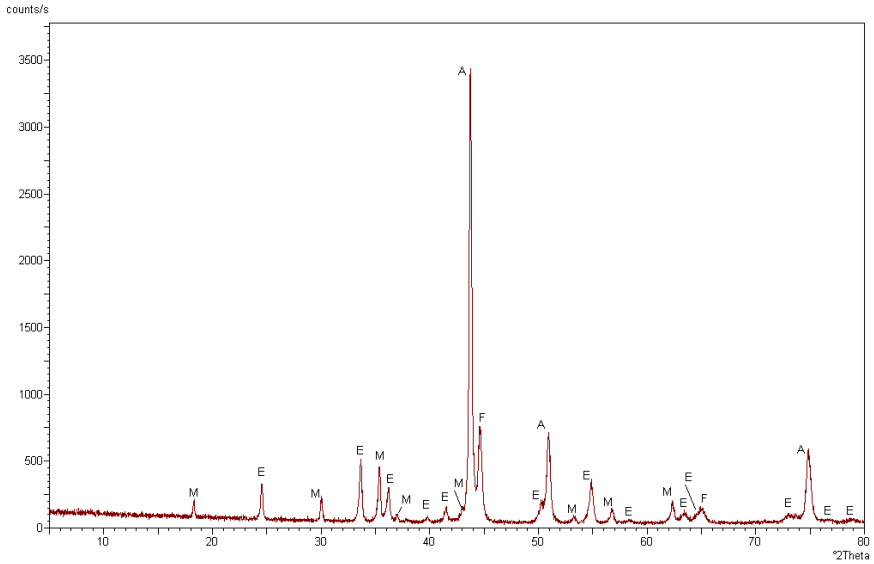

Fig. 4. XRD pattern for 316L outside surface exposed to air in single environment at 634 ^oC for 96 h (M-Fe_3O_4, E-Cr_2O_3, A-austenite, F-ferrite)

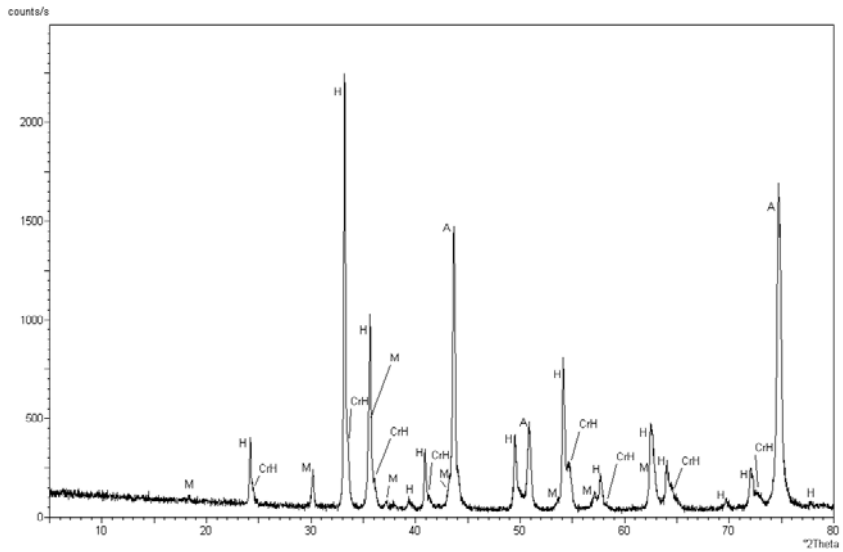

Fig. 5. XRD pattern for 316L inside surface exposed to air in single environment at 634 ^{o}C for 96 h (H-Fe_2O_3, CrH-$(Fe,Cr)_2O_3$, M-Fe_3O_4, A-austenite, F-ferrite)

Figure 6 shows the XRD pattern for outside (air) surface of the tubular specimen exposed to the dual environment. The phases identified in the scale are Fe_3O_4 spinel, Fe_2O_3, and Cr_2O_3. The phases identified in the scale on the inside surface exposed to H_2+3% H_2O were Fe_3O_4 and Cr_2O_3, Figure 7. The XRD results are summarized in Table 1.

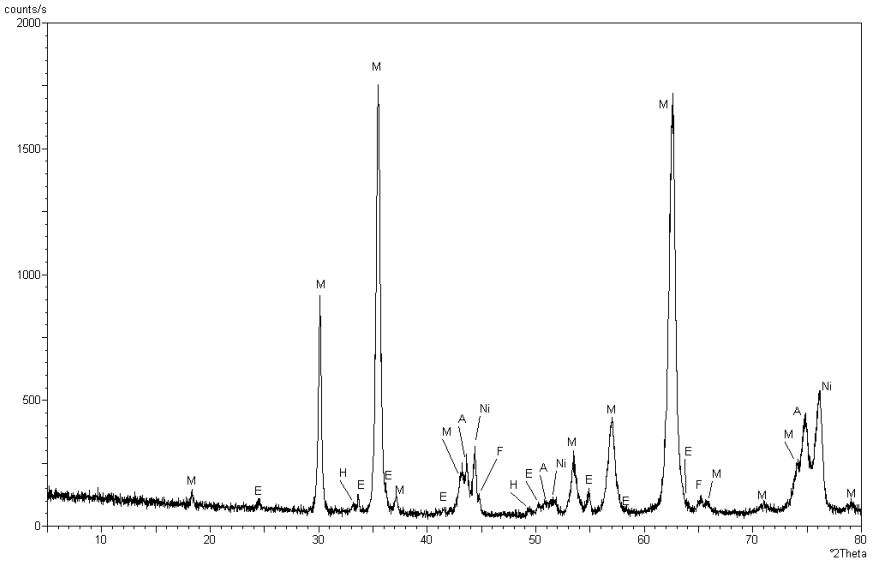

Fig. 6. XRD pattern for 316L outside surface exposed to air in dual environment at 634 ^{o}C for 96 h (M-Fe_3O_4, H-Fe_2O_3, E-Cr_2O_3, Ni- nickel, A-austenite, F-ferrite)

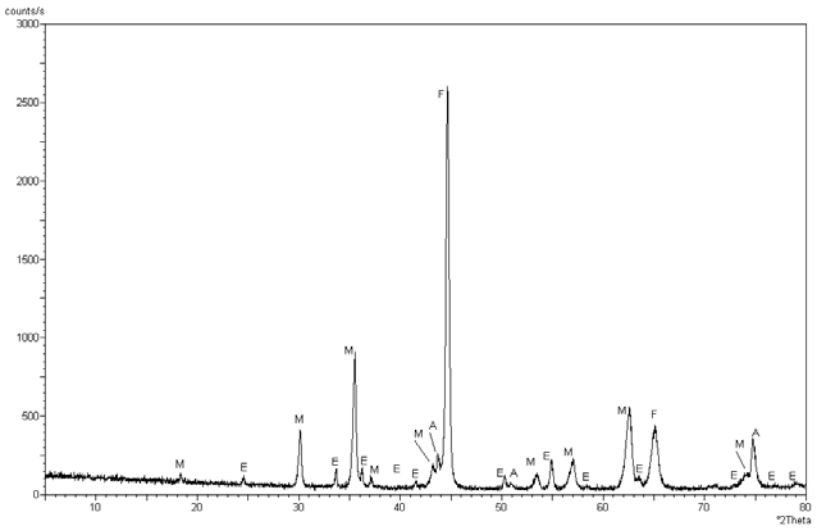

Fig. 7. XRD pattern for 316L inside surface exposed to H_2+3% H_2O in dual environment at 634 ^oC for 96 h(M-Fe_3O_4, E-Cr_2O_3, A-austenite, F-ferrite)

Table 1. XRD results of phases present in oxide scales formed on 316L at 634 ^oC for 96 h				
Environment	Relative Phase Amount			
	Primary	Secondary	Minor	Trace
Single - air (inside)	Fe_2O_3		$(Fe,Cr)_2O_3$	Fe_3O_4
Single - air (outside)			Fe_3O_4 Cr_2O_3	
Dual – H_2+3% H_2O side (inside)		Fe_3O_4	Cr_2O_3	
Dual - air side (outside)	Fe_3O_4			Fe_2O_3 Cr_2O_3

Raman spectroscopy analysis conducted at two locations on the outside surface of the tube specimens oxidized in the single environment confirmed the presence of a Cr_2O_3 and a spinel phase. The spinel phase peak was broader and at higher frequency than usual for Fe_3O_4 indicating that the spinel may also contain Ni or Cr, e.g. $NiCr_2O_4$ or $FeCr_2O_4$, in addition to Fe_3O_4. Results from the two locations showed different amounts of Cr_2O_3 and the spinel phase. The surface inside the tube appears to contain a mixture of α-Fe_2O_3 and a spinel phase. Again, the spinel phase does not appear to be pure Fe_3O_4, but rather a mixed spinel of the form $(Ni,Fe)(Cr,Fe)_2O_4$. The scale on the inside surface gives weaker signals than that on the outside, suggesting that the scale on the inside may be less crystalline.

Raman spectroscopy analysis was conducted at three locations on the outside surface of tube specimens oxidized in air in the dual environment. There was some variation in phase composition from one location to another. Some locations appear to have a thin scale of α-Fe_2O_3 and the mixed spinel $(Ni,Fe)(Cr,Fe)_2O_4$, while other locations appeared to be mostly the mixed spinel. The phase identified in the scale

formed inside the tube exposed to H_2+3% H_2O was mostly magnetite. The Raman spectroscopy results are summarized in Table 2.

It is worth noting that Fe_2O_3 is present in the scale formed inside the tube exposed in the single environment, but when hydrogen was present, as in the dual environment, Fe_2O_3 almost disappeared as shown in Figure 8.

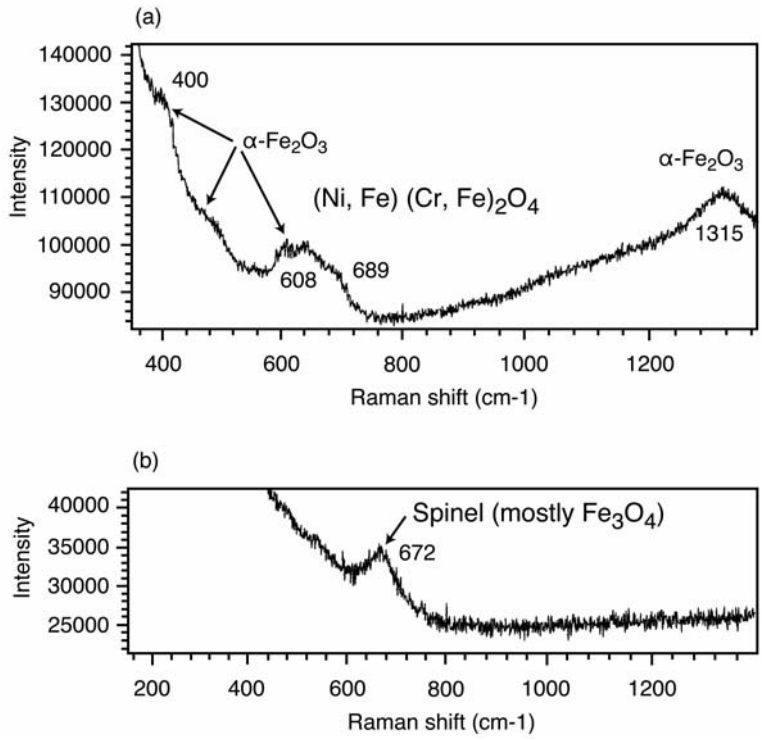

Fig. 8. Raman spectra for scale on inside surface of 316L tubes exposed to air from (a) single environment (air) and (b) dual environment (H_2+3% H_2O)

Table 2. Raman spectroscopy results of phases present in scales formed on 316L stainless at 634 °C for 96 h

Environment	Description	
	Crystalline Phases	Other
Single - air (inside)	Fe_2O_3 $(Ni,Fe)(Cr,Fe)_2O_4$ mixed spinel	
Single - air (outside)	Cr_2O_3 $(Ni,Fe)(Cr,Fe)_2O_4$ mixed spinel	
Dual – H_2 + 3% H_2O side (inside)	Fe_3O_4	Fe_2O_3 not present
Dual - air side (outside)	Fe_2O_3 $(Ni,Fe)(Cr,Fe)_2O_4$ mixed spinel	

In H_2+3% H_2O, the stable phase in the Fe-O-H system is Fe. Therefore, any Fe_2O_3 present would be reduced first to Fe_3O_4 and then to Fe. This is consistent with the results

in Figures 8. Raman spectroscopy is much more surface sensitive than XRD. Thus, comparison with the results in Figure 7 suggests that Fe_2O_3 was reduced to Fe_3O_4 on the outer surface (Figure 8) and remained unreacted deeper in the scale (Figure 7).

Electrical Properties

ASR is widely used to evaluate electrical properties of the oxide scales. It reflects both the conductivity and the thickness of the scale formed. [11, 12] Because of the way the measurements were made, the ASR values reported here are the total for the scale formed on the two sides of the sample. ASR can be expressed as:

$$ASR = (k_p't)^{1/2}\sigma^{-1} \quad (1)$$

where k_p' is the parabolic rate constant, σ is the conductivity of the oxide scale, and t is the exposure time in the oxidizing environment. The temperature dependence of oxide scale conductivity can be expressed by:

$$\sigma T = \sigma_0 e^{-E/RT} \quad (2)$$

where σ is conductivity, E is the activation energy of electrical conductivity, R is the gas constant, and T is the absolute temperature. Combining and rearranging terms yields:

$$1/ASR = \sigma_0 e^{-E/RT}/[T(k_p't)^{1/2}] \quad (3)$$

In this relationship, reciprocal ASR (which is proportional to conductivity) decreases with decreasing temperature. Figure 9 shows just such a relationship for the scale formed on 316L in the single and the dual environment as a function of reciprocal temperature. Thus, the scales are exhibiting temperature dependence that is typical of semiconductor

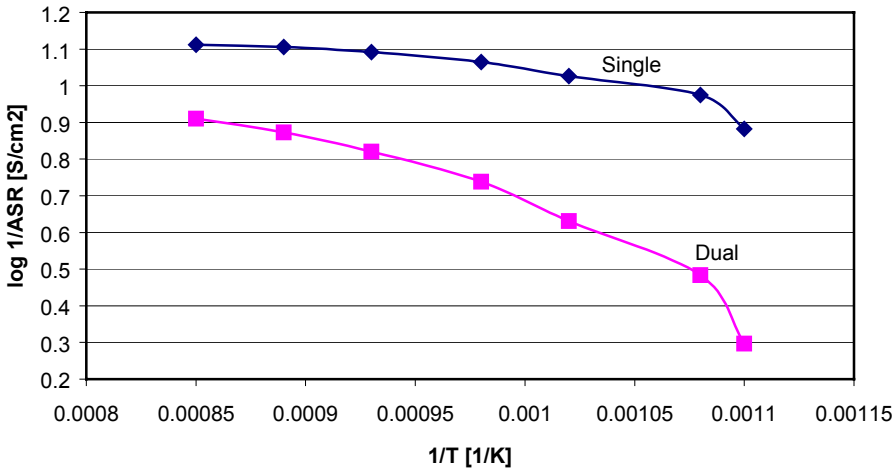

Fig. 9. Electrical conductivity of the scale formed on 316L exposed to the single and dual environments at 634 ^{o}C for 96 h

performance.[2] The electrical conductivity of the scale formed in the dual environment was lower than that formed in the single environment. The changes with temperature in the dual environment were more pronounced. This can be caused by differences in the defect structure of the semi-conducting phases such as Cr_2O_3.

SUMMARY AND CONCLUSIONS

The oxidation behavior of stainless steel in the single environment at 634 ^oC is different from that exposed to the dual environment. The microstructure and electrical conductivity temperature dependence of the scale formed in these two ways is different.

The main oxidation products in scaled formed in air were Fe-Ni-Cr spinels, Fe_2O_3, and Cr_2O_3. Those in the scale formed in H_2+3% H_2O were mainly of Fe_3O_4 and Cr_2O_3, with no evidence of Fe_2O_3.

The electrical conductivity temperature dependence of the scales formed in the single and dual environments both show semiconductor temperature dependence. Stainless steel oxidized in the single environment had a higher electrical conductivity than that oxidized in the dual environment.

ACKNOWLEDGEMENTS

The authors would like to thank Dr. Christopher Johnson and of the U.S. Department of Energy, National Energy Technology Laboratory and Mr. Chad Schaeffers (ORISE student) for their assistance in area-specific resistance measurements. Also, the authors are grateful to Mr. K. Collins, Mr. R.D. Govier and Dr. T. Adler of the U.S Department of Energy, Albany Research Center for their assistance and helpful discussions.

REFRENCES

1. L.Carrette, K.A. Friedrich and U. Stimming “Fuel-Cells-Fundamentals and Applications,” Fuel Cells, 2001, 1, p. 5

2. T. Horrita, Y. Xiong, K. Yamaji, N. Sakai, H. Yokokawa, J. Power Sources 118 (2003) 35-43.

3. W.A. Meulenberg, A. Gil, E. Wessel, H.P. Buchkremer, and D. Stöver “Corrosion and Interdiffusion in a Ni/Fe-Cr-Al Couple Used for the Anode Side of Multi-Layered Interconnector for SOFC Applications,” Oxidation of Metals, 57 (2002), 1-12.

4. Z.G Yang, K.S. Weil, D.M. Paxton, and J.W. Stevenson “Selection and Evaluation of Heat-Resistant Alloys for Planar SOFC Interconnect Applications,” Abstracts of 2002Fuel Cell Seminar, p. 522.

5. S. de Souza, S.J. Visco, L.C. De Jonghe, J. Electrochem. Soc., 144 (1997) L35.

6. P. Kofstad, Z. Hed, J. Electrochem. Soc., 116 (1969) 224.

7. P. Kofstad, Z. Hed, J. Electrochem. Soc., 116 (1969) 1542.

8. Prabhakar Singh & Z. Gary Yang, Thermo chemical analysis of Oxidation and Corrosion Processes in High Temperature Fuel Cells, Presented at 131st TMS Annual Meeting. Seattle, WA. February 18, 2002.

9. Z. Yang, K.S. Weil, M.S. Walker, P. Singh, Paxton, J.W. Stevenson, Electrochemical and Solid-State Letters, 6 (2003) 10.

10. M. Ziomek-Moroz, S.D. Cramer, G.H. Holcomb, B.S. Covino, Jr., A. Matthes, S.J. Bullard, J.S. Dunning, D.E. Alman, and Prabhakar Singh, 2003 Fuel Cell Seminar Abstracts, p. 522.

11. K. Huang, P. Y. Hou, J. B. Goodenough "Characterization of Iron-based Alloy Interconnect for Reduced Temperature Solid Oxide Fuel Cells," Solid State Ionics, 129 (2000) 237-250.

12. Z. Yang, K.S. Weil, D.M. Paxton, J.W. Stevenson, J. Electrochem. Soc., 150 (2003) A1188.